

A DECADE OF TIMING AN ACCRETION-POWERED MILLISECOND PULSAR: THE CONTINUING SPIN DOWN AND ORBITAL EVOLUTION OF SAX J1808.4–3658

JACOB M. HARTMAN^{1,2}, ALESSANDRO PATRUNO³, DEEPTO CHAKRABARTY⁴, CRAIG B. MARKWARDT^{5,6}, EDWARD H. MORGAN⁴, MICHIEL VAN DER KLIS³, RUDY WIJNANDS³

Accepted by ApJ

ABSTRACT

The *Rossi X-ray Timing Explorer* has observed five outbursts from the transient 2.5 ms accretion-powered pulsar SAX J1808.4–3658 during 1998–2008. We present a pulse timing study of the most recent outburst and compare it with the previous timing solutions. The spin frequency of the source continues to decrease at a rate of $(-5.5 \pm 1.2) \times 10^{-18}$ Hz s⁻¹, which is consistent with the previously determined spin derivative. The spin-down occurs mostly during quiescence, and it is most likely due to the magnetic dipole torque from a $B = 1.5 \times 10^8$ G dipolar field at the neutron star surface. We also find that the 2 hr binary orbital period is increasing at a rate of $(3.80 \pm 0.06) \times 10^{-12}$ s s⁻¹, also consistent with previous measurements. It remains uncertain whether this orbital change reflects secular evolution or short-term variability.

Subject headings: binaries: general — stars: individual (SAX J1808.4–3658) — stars: neutron — stars: rotation — X-rays: binaries — X-rays: stars

1. INTRODUCTION

Ten years ago, observations of the recurrent X-ray transient SAX J1808.4–3658 with the *Rossi X-ray Timing Explorer* (*RXTE*) revealed coherent 2.5 ms pulsations, establishing this source as the first known accretion-powered millisecond pulsar (AMP; Wijnands & van der Klis 1998). Its immediate recognition as the “missing link” in which old pulsars are spun up to millisecond periods by accretion in an X-ray binary was only the beginning of what can be learned from this class of sources: among other areas of theoretical interest, AMPs continue to reveal insights into the nature of magnetically channeled accretion flow, the torques that act upon neutron stars in low-mass X-ray binaries (LMXBs), and the orbital evolution of these systems. This paper investigates the 2008 October X-ray outburst of SAX J1808.4–3658, which touches upon all these questions.

SAX J1808.4–3658 was originally discovered by the *BeppoSAX* WFC monitor during a 1996 outburst (in ‘t Zand et al. 1998, 2001). It was the first LMXB known to exhibit all three modes of millisecond X-ray variability established by the *RXTE*: accretion-powered pulsations (Wijnands & van der Klis 1998), X-ray burst oscillations (Chakrabarty et al. 2003), and kilohertz quasi-periodic oscillations (Wijnands et al. 2003). The source has been extensively studied for over 1.7 Ms with the *RXTE* PCA during outbursts in 1998, 2000,

2002, 2005, and 2008, making it the best-studied AMP. Its outbursts rise from quiescence ($L_{\text{bol}} \lesssim 10^{32}$ erg s⁻¹; Campana et al. 2002; Heinke et al. 2007) to their peak fluxes in ≈ 5 d, followed by ≈ 5 d at peak bolometric luminosities of $L_{\text{bol}} = (5-8) \times 10^{36}$ erg s⁻¹ (for a distance of 3.5 kpc and the bolometric correction given by Galloway & Cumming 2006), ≈ 15 d of decay back to near-quiescent fluxes, and a month or more of low-luminosity flaring (Hartman et al. 2008a, hereafter H08). These outbursts recur every 1.6–3.3 years.

Orbital modulation of the persistent pulsations establishes a 2.01 hr binary orbital period (Chakrabarty & Morgan 1998). Its mass donor is likely an extremely low-mass ($\approx 0.05 M_{\odot}$) brown dwarf (Bildsten & Chakrabarty 2001). The system has been detected and extensively studied in the optical (Roche et al. 1998; Giles et al. 1999; Wang et al. 2001; Deloye et al. 2008; Wang et al. 2008), and its relatively high optical luminosity during X-ray quiescence has led to speculation that the neutron star (NS) may be an active radio pulsar during these intervals (Homer et al. 2001; Burderi et al. 2003; Campana et al. 2004), although radio pulsations have not been detected (Burgay et al. 2003). Pulse timing of the four outbursts during 1998–2005 revealed that the spin frequency of SAX J1808.4–3658 is decreasing during quiescence at a rate of $\dot{\nu} = (-5.6 \pm 2.0) \times 10^{-16}$ Hz s⁻¹, while its orbital period is increasing at a rate of $\dot{P}_{\text{orb}} = (3.5 \pm 0.2) \times 10^{-12}$ s s⁻¹ (H08; Di Salvo et al. 2008).

2. X-RAY OBSERVATIONS AND ANALYSIS

Routine monitoring of the Galactic bulge region with the *RXTE* PCA revealed SAX J1808.4–3658 to again be in outburst on 2008 Sep 21 (Markwardt & Swank 2008). *RXTE* observed the source almost every day during the outburst, producing 270 ks of data with 122 μ s time resolution and 64 energy channels covering the 2–60 keV range of the PCA. Unfortunately, the total effective area of the PCA has decreased significantly since the earlier

¹ Space Science Division, Naval Research Laboratory, Washington, DC 20375, USA; jacob.hartman@nrl.navy.mil

² National Research Council Research Associate

³ Astronomical Institute “Anton Pannekoek,” University of Amsterdam, Kruislaan 403, 1098 SJ Amsterdam, Netherlands; a.patruno, m.b.m.vanderklis, r.a.d.wijnands@uva.nl

⁴ Department of Physics and Kavli Institute for Astrophysics and Space Research, Massachusetts Institute of Technology, Cambridge, MA 02139; deepto, ehm@space.mit.edu

⁵ CRESST/Department of Astronomy, University of Maryland, College Park, MD 20742

⁶ Astrophysics Science Division, NASA Goddard Space Flight Center, Greenbelt, MD 20771; craigm@milkyway.gsfc.nasa.gov

outbursts: an average of only 1.8 of the 5 proportional counter units are on during these observations, resulting in a mean effective area of 2200 cm^2 .

Our analysis followed the techniques developed in H08 and applied to the earlier outbursts of SAX J1808.4–3658. We shifted the photon arrival times to the solar system barycenter using the optical position from H08, applied the *RXTE* fine clock correction, and filtered out data during Earth occultations and intervals of unstable pointing. We also removed data from 1 min before to 10 min after the two thermonuclear X-ray bursts observed by the *RXTE* during this outburst.

To measure the times of arrival (TOAs) and fractional amplitudes of the persistent pulsations, we folded 512 s intervals of data using a preliminary timing model based on extrapolating forward the H08 results. The timing models were applied and fitted using the TEMPO pulse timing program, version 11.005,⁷ and assumed a circular orbit and a fixed spin frequency. From the resulting folded pulse profiles, we measured the phases and amplitudes of the fundamental and the second harmonic of the pulsation.⁸ Higher harmonics had insufficient power to be useful for pulse phase timing.

Special care must be taken when measuring the pulse TOAs for SAX J1808.4–3658. As in past outbursts, the harmonic phase residuals relative to our best timing models exhibit variability on time scales of ~ 10 hr and longer that is well in excess of the Poisson noise expected from counting statistics. As described in H08, we applied a frequency-domain filter that weighs the harmonics according to observed noise properties in order to generate a minimum-variance estimator of the NS spin phase. For this outburst, the second harmonic had less excess timing noise, so it was weighted more heavily when estimating the overall pulse TOAs. With these pulse TOA estimates, we used TEMPO to fit an improved timing model. By iteratively re-folding the data, estimating the pulse TOAs, and fitting a new model, we converged on our best-fit timing model.

Uncertainties in our frequency measurements were estimated using Monte Carlo simulations, following the prescription of H08. These simulations account for the impact of long-time-scale correlations in the pulse arrival times. To test for the presence of a frequency derivative, we fit one to the pulse TOAs and estimated its significance with our simulations.

To measure the orbital period and its derivative, we connected the orbital phases of all the outbursts. The uncertainty in the 2008 orbital phase was estimated by measuring and accounting for the timing noise at scales of $\lesssim P_{\text{orb}}$; as in previous outbursts (H08), the noise was close to white but somewhat higher than what would be expected from Poisson noise alone.

3. RESULTS

In most respects, the 2008 outburst of SAX J1808.4–3658 continues the trends and patterns observed during the earlier outbursts. Figure 1 shows its light curve, pulse phases, and fractional amplitudes, along with six representative 2–15 keV pulse

profiles.

The light curve of the main body of the outburst is remarkably similar the light curve observed in 2005, which is included in Figure 1 for comparison. The 2008 outburst is slightly dimmer (maximum 2.5–25 keV flux of $(1.74 \pm 0.02) \times 10^{-9} \text{ erg cm}^{-2} \text{ s}^{-1}$) and its light curve has two maxima, but the outburst rise, the length of the peak, and the slow decay down to $\approx 4 \times 10^{-10} \text{ erg cm}^{-2} \text{ s}^{-1}$ are nearly identical.

The flaring tail of the new outburst is markedly dimmer. During the two previous outbursts for which the tail was observed immediately following the main outburst (2002 and 2005), the flares were quasiperiodic with a 4–6 d time scale, and the 2.5–25 keV flux varied between $\sim 10^{-11} \text{ erg cm}^{-2} \text{ s}^{-1}$ and $4 \times 10^{-10} \text{ erg cm}^{-2} \text{ s}^{-1}$. The source remained consistently detectable for at least a month following the main outburst. In contrast, the brightest observations during the tail of the 2008 outburst only reach $2.5 \times 10^{-10} \text{ erg cm}^{-2} \text{ s}^{-1}$, and during Oct 13–17, the source was not detectable at all with the *RXTE* ($\sim 10^{-11} \text{ erg cm}^{-2} \text{ s}^{-1}$ sensitivity). This behavior is similar to the intermittent detections during the tail of the 2000 outburst (Wijnands et al. 2001).

Most of the pulse profiles were similar to what we observed during the earlier outbursts: profiles 1–3 of Figure 1 closely resemble profiles 1–3 in Figure 3 of H08. The evolution of the pulse shape progresses in the same way. As seen in the 2005 and (to a lesser extent) 2002 outbursts, a symmetric pulse during the burst rise becomes increasingly skewed during the burst peak. In the phase residuals, this pulse shape change manifests as a progressively increasing phase of the fundamental, while the phase of the second harmonic remains constant; this behavior can be seen during MJD 54732–54735 in the phase offset plot of Figure 1. Since these pulse shape changes confuse measurement of the spin phase, we omit the outburst rise and early peak (points before MJD 54735) from our timing models. This choice is admittedly somewhat arbitrary, as the pulse profile continues to change throughout the outburst, albeit more slowly. However, this same region was omitted from the analysis of the earlier outbursts in H08, so we remove it here so that our frequency measurements are directly comparable.⁹

The clear double peaks of profile 4 are an exception to these similarities in the pulse shape evolution. This profile folds 8.2 ks of data during MJD 54743.2–54744.0. It occurs during the slow-decay stage of the outburst, at a 2.5–25 keV flux of $1.0 \times 10^{-9} \text{ erg cm}^{-2} \text{ s}^{-1}$. In none of the earlier outbursts was a second peak so prominent, and the weak secondary peaks that were observed occurred exclusively during the flaring tail, when the source was a factor of 2–3 dimmer.

The most unusual timing feature of this outburst is the presence of abrupt shifts of the fundamental’s phase during the outburst tail. These phase jumps are clear at MJD 54770 and 54774 in the phase offset plot of Figure 1, at which times the fundamental phases are 0.2–0.3 cycles

⁹ Including the phases during the outburst rise decreases the frequencies cited throughout this paper by 20–30 nHz. Including this stage in the earlier outbursts causes their measured frequencies to shift similarly, so the value of the long-term spin down is not affected.

⁷ At <http://www.atnf.csiro.au/research/pulsar/tempo>

⁸ Throughout this paper, we number the harmonics such that the k th harmonic is k times the frequency of the 401 Hz fundamental.

earlier than predicted by the constant-frequency model shown. The observations with earlier phases were folded and summed to produce profile 6, and their phases are marked by circles. The rest of the observations in the tail were folded to produce profile 5, and after MJD 54760 their phases are marked by squares. While substantial phase shifts have been observed in the previous outbursts of SAX J1808.4–3658 (compare Fig. 2 of Burderi et al. 2006 and Fig. 1 of H08), these jumps were particularly large and rapid. During the 23 hours between the observations on MJD 54770 and 54771, the phase shifted by 0.26 cycles; during the single observation on MJD 54775, the phase shifted by 0.20 cycles in 40 minutes. These shifts are due in part to differing pulse shapes. The centroid of the pulse — to which the fundamental is most sensitive — arrives appreciably earlier in profile 6, but the peaks of the two profiles are separated by a smaller difference. However, this nuance is lost unless many observations are folded together (as in the displayed profiles), and for most observations in the tail only the fundamental is available for pulse timing.

Given this limitation, the inclusion of these phase measurements of the fundamental in our timing models is subject to interpretation. If these points are all excluded, the phase residuals for MJD 54735–54760 give a frequency of 400.97521012(3) Hz. (Parenthetical digits give 1 σ estimates of the uncertainties.) If the circled points are used and the square points excluded, the timing solution requires a large apparent spin up to account for the advancing phases in the outburst tail. Its frequency rises at a rate $\dot{\nu} = (1.1 \pm 0.2) \times 10^{-13}$ Hz s⁻¹ from a value of $\nu_{\text{start}} = 400.97521002(5)$ at the start of the outburst. This fit is indicated by the dotted line in the phase offset panel of Figure 1. It does not completely eliminate the jumps: a substantial difference (0.16 cycles) remains between the points around MJD 54770 and 54774. On the other hand, if we only include the square points in the outburst tail, the data are consistent with a constant spin frequency of 400.97521013(2) Hz. This selection eliminates all phase jumps greater than 0.1 cycles. Finally, if we include all the points in the tail, we get $\dot{\nu} = 0.6(4) \times 10^{-13}$ Hz s⁻¹ and $\nu_{\text{start}} = 400.97521009(6)$, although the phase jumps result in a poor fit and large uncertainties.

Ultimately we are most interested in these frequency measurements to determine whether the long-term spin down observed in H08 has continued, and on this point the data are clear: regardless of our assumptions, the estimated spin frequency at the start of the 2008 outburst is less than the 2005 frequency of 400.97521019(2) Hz (H08). Fitting a constant slope through the frequencies observed for the five outbursts yields a long-term spin-down rate of $\dot{\nu} = (-5.5 \pm 1.2) \times 10^{-16}$ Hz s⁻¹, as shown in the top panel of Figure 2. This rate and figure use the 2008 timing model obtained when we only include the square points; we prefer this model on physical grounds (see §4.1). That said, using the ν_{start} frequency from the model for only the circled points does not greatly alter the result, slightly increasing its magnitude to -6.2×10^{-16} Hz s⁻¹. However, the 2008 point becomes an outlier and the χ^2 of the fit increases.

These values are in excellent agreement with the spin down of $(-5.6 \pm 2.0) \times 10^{-16}$ Hz s⁻¹ found for the 1998–2005 outbursts (H08). The frequency uncertainties esti-

TABLE 1
COMBINED TIMING PARAMETERS FOR SAX J1808.4–3658

Orbital period, P_{orb} (s) ^a	7249.156980(4)
Orbital period derivative, \dot{P}_{orb} (10^{-12} s s ⁻¹)	3.80(6)
Projected semimajor axis, $a_x \sin i$ (light-ms)	62.812(2)
Time of ascending node, T_{asc} (MJD, TDB)	52499.9602472(9)
Eccentricity, e (95% confidence upper limit)	$< 1.2 \times 10^{-4}$
Spin frequency, ν (Hz) ^a	400.975210240(9)
Spin frequency derivative, $\dot{\nu}$ (10^{-16} Hz s ⁻¹)	-5.5(1.2)

^a P_{orb} and ν are specified for the time T_{asc} (2002 Aug 14.0).

mated using our Monte Carlo simulations give $\chi^2 = 9.7$ with 3 degrees of freedom. To account for this large χ^2 , we scaled up the frequency uncertainties such that the reduced χ^2 is unity when calculating the uncertainty for $\dot{\nu}$. The fit is not particularly sensitive to the source position: shifting it by 1 σ along the ecliptic (using the uncertainty from the optical position in H08) changes the spin down by 0.2×10^{-16} Hz s⁻¹. No position significantly decreases the χ^2 of the linear trendline.

The farthest outlier from a constant frequency derivative is the 2000 outburst, of which we only observed the flaring tail. As noted in H08, this frequency measurement may be complicated by small systematic differences in the observed pulse frequency between the main outburst and its tail, which were observed during the 1998 and 2002 outbursts. Removing this outburst lowers the χ^2 to 1.9 (2 degrees of freedom), consistent with a constant derivative, and changes the long-term spin down to $(-6.5 \pm 0.8) \times 10^{-16}$ Hz s⁻¹.

The measured time of ascending node¹⁰ continues to advance relative to a constant orbital period. A quadratic provides a good fit ($\chi^2 = 2.9$ with 2 degrees of freedom), consistent with a constant orbital period derivative of $\dot{P}_{\text{orb}} = (3.80 \pm 0.06) \times 10^{-12}$ s s⁻¹. This measurement is 1.5 σ greater than the value in H08. It is in good agreement with Burderi et al. (2009), which measured the orbital phase of the 2008 outburst using *XMM-Newton* data. All other orbital parameters differ by less than 1 σ from the values listed in H08. Table 1 summarizes all the parameters for the long-term pulse timing of SAX J1808.4–3658.

Proper interpretation of the phase residuals hinges on an accurate handling of the orbital parameters, particularly the orbital period, due to the sparsity of data in the outburst’s tail. From the orbital parameters derived by connecting the advancing orbital phases of the 1998–2005 outbursts (H08), we extrapolate a 2008 orbital period of 7249.15763(6) s. Including the 2008 outburst’s phase, this method gives 7249.15771(2) s. Fitting the orbital parameters using the fundamental for the first half of the outburst only (cf. Patruno et al. 2008) or using only the second harmonic give compatible periods of 7249.160(3) s and 7249.153(5) s, respectively. However, fitting to the phase of the fundamental over the entire outburst yields a period of 7249.174(2) s, 9 σ higher than the far more accurate values derived through phase connection. Because the phase measurements in the outburst tail are sparse due to the source’s highly variable flux, their coverage

¹⁰ The ascending node is the point of zero degrees true longitude, which is the same as zero degrees mean longitude for a circular orbit like this one.

of the orbital phase is limited, and TEMPO attempts to “correct” for the observed jumps by over-fitting P_{orb} .

4. DISCUSSION

4.1. The double-peaked pulse profiles and phase jumps

The presence of double-peaked pulse profiles during the 2008 outburst was notable both because two peaks were so well defined (compare with the weaker secondary peaks shown in Fig. 3 of H08) and because they occurred while the outburst was still relatively bright: 2–3 times more luminous than when double-peaked profiles were first seen during the 2002 and 2005 outbursts. H08 speculated that the appearance of a second peak may be caused by the recession of the accretion disk as the accretion rate drops, revealing the star’s antipodal hot spot. Ibragimov & Poutanen (2009) went further, estimating from magnetic accretion theory and geometric considerations that the appearance of the antipodal hot spot at fluxes of $F_{\text{bol}} \approx 0.8 \times 10^{-9} \text{ erg cm}^{-2} \text{ s}^{-1}$ during 2002 and 2005 would imply a surface magnetic field of $B \approx (0.4\text{--}1.2) \times 10^8 \text{ G}$.

The detection of double-peaked profiles at $F_{\text{bol}} = 2.1 \times 10^{-9} \text{ erg cm}^{-2} \text{ s}^{-1}$ during 2008 requires this field estimate to be increased somewhat, although its weak dependence on flux ($\propto F^{1/2}$ in eq. 14 of Ibragimov & Poutanen 2009) means that is still not in conflict with the $B \leq 1.5 \times 10^8 \text{ G}$ limit implied by the long-term spin down (H08; see also §4.2). More troublesome is the question of why the second spot does not remain visible as the accretion rate continues to drop. It is difficult to imagine a change in the geometry or inner radius of the disk that temporarily reveals the antipodal hot spot but has no impact at all on the accretion rate and flux, as is the case here. More exotic explanations, such as a temporary bifurcation of the accretion column to produce two hot spots, may be needed; simulations have suggested that such configurations are easily possible if higher-order field components are present (Long et al. 2008).

The large phase jumps in the tail of the 2008 outburst are the most unusual feature of the pulse profiles, with the phase of the fundamental in one case jumping by 0.20 cycles in only 40 minutes. Clearly these are not changes in the rotational phase of the NS, which complicates their inclusion while constructing a timing solution. We considered two extremes: that the earlier points reflected the NS spin phase, which necessitated a spin up of $1.1(2) \times 10^{-13} \text{ Hz s}^{-1}$; and that the later points tracked the spin, in which case a constant-frequency timing solution provides a good fit.

We prefer the latter case on physical grounds. From standard magnetic accretion torque theory (e.g., Pringle & Rees 1972), an accretion rate of \dot{M} can impart a maximum torque of $2\pi I \dot{\nu} \leq \dot{M}(GM r_{\text{co}})^{1/2}$, where r_{co} is the co-rotation radius of the NS and I is its moment of inertia. Estimating $\dot{M} = L_{\text{bol}}(GM/R)^{-1}$, we find the maximum spin up of

$$\begin{aligned} \dot{\nu} \leq & 6 \times 10^{-14} \left(\frac{F_{2.5-25 \text{ keV}}}{1 \times 10^{-9} \text{ erg cm}^{-2} \text{ s}^{-1}} \right) \left(\frac{c_{\text{bol}}}{2.12} \right) \times \\ & \left(\frac{d}{3.5 \text{ kpc}} \right)^2 \left(\frac{I}{10^{45} \text{ g cm}^2} \right)^{-1} \left(\frac{R}{10 \text{ km}} \right) \times \\ & \left(\frac{M}{1.4 M_{\odot}} \right)^{-1/3} \left(\frac{\nu}{401 \text{ Hz}} \right)^{-1/3} \text{ Hz s}^{-1} \quad (1) \end{aligned}$$

Here we use the bolometric correction c_{bol} and distance d from Galloway & Cumming (2006) and canonical values for the NS parameters. Integrating this expression for the observed flux over the 40 d outburst, we can approximate a physical upper limit for the total spin up of $\Delta\nu \leq 0.12 \mu\text{Hz}$. For the earlier points to reflect the spin phase, the frequency shift would need to be $\Delta\nu = 1.1 \times 10^{-13} \text{ Hz s}^{-1} \cdot 40 \text{ d} = 0.38 \mu\text{Hz}$. Unless the source’s luminosity underestimates the accretion rate by a factor of a few, these points cannot reflect the NS spin phase.

Of course, it is possible that the NS spin phase lies somewhere between these two extremes. Based on the data available, we cannot exclude the possibility of a spin up during the outburst. Indeed, though the confidence intervals in 1998–2005 include zero, they are biased toward a positive $\dot{\nu}$ (H08), suggestive that a small systematic spin up may be present.

4.2. Interpreting the spin frequency derivative

The observed long-term spin down of SAX J1808.4–3658 produces a loss of rotational energy at a rate of $\dot{E}_{\text{sd}} = 4\pi^2 I \nu \dot{\nu} = -9 \times 10^{33} \text{ erg s}^{-1}$, assuming a canonical value of $I = 10^{45} \text{ g cm}^2$ for the NS moment of inertia. This spin down acts on the NS during quiescence (H08), and it is consistent with a constant rate over the ten years of observation. We consider three possible torques: magnetic dipole radiation, the centrifugal expulsion of matter from the inner accretion disk by the magnetic field (the so-called “propeller effect”), and gravitational radiation due to a mass quadrupole moment of the NS. We assume that these independent mechanisms contribute additively to the observed spin-down luminosity, $\dot{E}_{\text{sd}} = \dot{E}_{\text{dipole}} + \dot{E}_{\text{prop}} + \dot{E}_{\text{gr}}$.

The presence of pulsations during the outburst peaks requires $B > 0.4 \times 10^8$ to truncate the accretion flow above the NS surface (Psaltis & Chakrabarty 1999; H08). This lower limit implies a magnetic dipole contribution of $\dot{E}_{\text{dipole}}/\dot{E}_{\text{sd}} > 10\%$. If the field strength is only a few times higher, $B = 1.5 \times 10^8 \text{ G}$, then magnetic dipole radiation would account for the entirety of the long-term spin down. These tight limits on B leave a very small window for other mechanisms. Their contribution would have to be within a single order of magnitude of the contribution from magnetic dipole radiation. Given the wide physical ranges available to these independent spin-down torques, such a coincidence is unlikely. Additionally, the long-term spin down is consistent with a constant rate, as would be expected if \dot{E}_{dipole} dominates; the constancy of \dot{E}_{prop} and \dot{E}_{gr} is very model dependent.

Independent estimates of the magnetic field strength suggest that B is toward the upper end of our allowed interval. Gilfanov et al. (1998) noted that if the rapid dimming at the end of the main outburst is due to the onset of the propeller effect (as suggested by other outburst properties, e.g., Hartman et al. 2008b), it would imply $B \sim 1 \times 10^8 \text{ G}$. As noted in the previous section, the appearance of double-peaked pulse profiles in the tail suggest a similar field strength (Ibragimov & Poutanen 2009). The detection of a relativistically broadened iron line during the 2008 outburst also suggests a higher field of $(3 \pm 1) \times 10^8 \text{ G}$ (Cackett et al. 2009; Papitto et al. 2009). For all these reasons, it is likely that magnetic dipole radiation provides the dominant torque.

4.3. Interpreting the orbital period derivative

The cause of the orbital period derivative remains a subject of debate. H08, Di Salvo et al. (2008), and Burderi et al. (2009) show that it cannot be accounted for solely by conservative transfer from the low-mass companion to the NS. We consider two alternatives: the ejection of mass from the system due to the ablation of the companion, and the influence of short-term effects that can exchange angular momentum between the companion and the orbit.

Ejection of matter due to the ablation of the companion. If magnetic dipole torque is the predominant contributor to the spin down of SAX J1808.4–3658, as suggested in the previous section, then the source may behave like a rotation-powered pulsar during quiescence, producing radio pulsations and a particle wind. While no radio pulsations have been detected (Burgay et al. 2003), the upper limits are not particularly constraining. However, during quiescence the system is substantially brighter in the optical than expected (Homer et al. 2001). This optical excess may be due to the heating of the companion by a particle wind (Burderi et al. 2003).

If this particle wind ejects a large amount of matter from the system, it could explain the rapid orbital period change. For a companion modeled with a polytropic index of $n = 3/2$ (representative of a degenerate or fully convective star), a mass loss of $\sim 10^{-9} M_{\odot} \text{ yr}^{-1}$ would be needed to yield the observed \dot{P}_{orb} (Di Salvo et al. 2008).

Is the spin-down luminosity of $\dot{E}_{\text{sd}} = -9 \times 10^{33} \text{ erg s}^{-1}$ sufficient to drive such mass loss? Assuming that it is radiated isotropically, the incident luminosity onto the companion is $\dot{E}_{\text{abl}} = -\frac{1}{4}(R_c/a)^2 \dot{E}_{\text{sd}}$, where R_c is the companion radius and a is the binary separation. Since the companion fills its Roche lobe, $R_c/a \approx 0.15$ for a mass ratio of $q \approx 0.05/1.4$ (Eggleton 1983). The resulting luminosity onto the companion is $\dot{E}_{\text{abl}} = 2.1 \times 10^{32} \text{ erg s}^{-1}$. Assuming perfect efficiency, that incident luminosity can drive a mass loss of $\dot{M}_c = -\dot{E}_{\text{abl}} R_c / GM_c = -1.2 \times 10^{-9} M_{\odot} \text{ yr}^{-1}$. Thus this scenario for orbital evolution is energetically feasible.

Nevertheless, some serious problems with this model remain. A particle wind sufficient to eject over 95% of \dot{M}_c from the system, as necessitated by this model, would also drive away the accretion disk. Di Salvo et al. (2008) suggest that outbursts therefore occur when the pressure of matter driven from the companion temporarily exceeds the radiation pressure. However, the outburst of SAX J1808.4–3658 and the other AMPs look quite sim-

ilar to some of the outbursts from other LMXBs, both in time scales and shape. The disk instability model has been generally successful in explaining the light curves of soft X-ray transients in general (e.g., King & Ritter 1998) and AMPs in particular (Powell et al. 2007). It is difficult to reconcile these similarities in light curve shape and time scale with a very different mechanism governing the outbursts of SAX J1808.4–3658.

Short-term changes in the orbital period. Alternatively, the observed \dot{P}_{orb} may not be representative of the secular evolution, but is instead due to some short-term interchange of angular momentum between the companion and the orbit. Similarly large orbital period derivatives are present in two so-called “black widow” millisecond radio pulsars, and these period derivatives have been observed to change sign on a ~ 10 yr time scale (Arzoumanian et al. 1994; Doroshenko et al. 2001). It has been suggested that tidal dissipation and magnetic activity in the companion are responsible for the orbital variability, requiring that the companion is at least partially non-degenerate, convective, and magnetically active (Arzoumanian et al. 1994; Applegate & Shaham 1994; Doroshenko et al. 2001). Eclipse timing of the LMXB EXO 0748–676 also shows rapid variation in the orbital period; explanations for the exchange of angular momentum include a “wobble” of the companion’s inertial moments due to differential rotation and convection produced by its uneven heating (Wolff et al. 2002).

However, in all the above systems, the orbital period derivatives change over $\lesssim 10$ yr. While this does not definitively prove that the \dot{P}_{orb} of SAX J1808.4–3658 is secular, it would make this source an exception. In contrast, the spin-down rate of the ablation model should be constant, so it is supported by the data from the 2008 outburst.

We are grateful to Jean Swank and the *RXTE* operations team at NASA Goddard Space Flight Center for their help in scheduling these observations. We also thank Tiziana Di Salvo, Luciano Burderi, Duncan Galloway, and Mike Wolff for useful discussions. We thank the referee for useful suggestions. This work was supported in part by NASA grants NNX07AP93G and NNX08AJ43G, awarded to MIT through the *RXTE* Guest Observer Program and the Astrophysics Data Program.

REFERENCES

- Applegate, J. H. & Shaham, J. 1994, *ApJ*, 436, 312
 Arzoumanian, Z., Fruchter, A. S., & Taylor, J. H. 1994, *ApJ*, 426, L85
 Bildsten, L. & Chakrabarty, D. 2001, *ApJ*, 557, 292
 Burderi, L., Di Salvo, T., D’Antona, F., Robba, N. R., & Testa, V. 2003, *A&A*, 404, L43
 Burderi, L., Di Salvo, T., Menna, M. T., Riggio, A., & Papitto, A. 2006, *ApJ*, 653, L133
 Burderi, L., Riggio, A., Di Salvo, T., Papitto, A., Menna, M. T., D’Aí, A., & Iaria, R. 2009, *A&A*, submitted, arXiv: 0902.2128
 Burgay, M., Burderi, L., Possenti, A., D’Amico, N., Manchester, R. N., Lyne, A. G., Camilo, F., & Campana, S. 2003, *ApJ*, 589, 902
 Cackett, E. M., Altamirano, D., Patruno, A., Miller, J. M., Reynolds, M., Linares, M., & Wijnands, R. 2009, *ApJ*, accepted, arXiv: 0901.3142
 Campana, S., D’Avanzo, P., Casares, J., Covino, S., Israel, G., Marconi, G., Hynes, R., Charles, P., & Stella, L. 2004, *ApJ*, 614, L49
 Campana, S., Stella, L., Gastaldello, F., Mereghetti, S., Colpi, M., Israel, G. L., Burderi, L., Di Salvo, T., & Robba, N. R. 2002, *ApJ*, 575, L15
 Chakrabarty, D. & Morgan, E. H. 1998, *Nature*, 394, 346
 Chakrabarty, D., Morgan, E. H., Munro, M. P., Galloway, D. K., Wijnands, R., van der Klis, M., & Markwardt, C. B. 2003, *Nature*, 424, 42

- Deloye, C. J., Heinke, C. O., Taam, R. E., & Jonker, P. G. 2008, *MNRAS*, 391, 1619
- Di Salvo, T., Burderi, L., Riggio, A., Papitto, A., & Menna, M. T. 2008, *MNRAS*, 389, 1851
- Doroshenko, O., Löhmer, O., Kramer, M., Jessner, A., Wielebinski, R., Lyne, A. G., & Lange, C. 2001, *A&A*, 379, 579
- Eggleton, P. P. 1983, *ApJ*, 268, 368
- Galloway, D. K. & Cumming, A. 2006, *ApJ*, 652, 559
- Giles, A. B., Hill, K. M., & Greenhill, J. G. 1999, *MNRAS*, 304, 47
- Gilfanov, M., Revnivtsev, M., Sunyaev, R., & Churazov, E. 1998, *A&A*, 338, L83
- Hartman, J. M., Patruno, A., Chakrabarty, D., Kaplan, D. L., Markwardt, C. B., Morgan, E. H., Ray, P. S., van der Klis, M., & Wijnands, R. 2008a, *ApJ*, 675, 1468 (H08)
- Hartman, J. M., Watts, A. L., & Chakrabarty, D. 2008b, *ApJ*, submitted, arXiv: 0809.3722
- Heinke, C. O., Jonker, P. G., Wijnands, R., & Taam, R. E. 2007, *ApJ*, 660, 1424
- Homer, L., Charles, P. A., Chakrabarty, D., & van Zyl, L. 2001, *MNRAS*, 325, 1471
- Ibragimov, A. & Poutanen, J. 2009, *MNRAS*, submitted, arXiv: 0901.0073
- in 't Zand, J. J. M., Cornelisse, R., Kuulkers, E., Heise, J., Kuiper, L., Bazzano, A., Cocchi, M., Muller, J. M., Natalucci, L., Smith, M. J. S., & Ubertini, P. 2001, *A&A*, 372, 916
- in 't Zand, J. J. M., Heise, J., Muller, J. M., Bazzano, A., Cocchi, M., Natalucci, L., & Ubertini, P. 1998, *A&A*, 331, L25
- King, A. R. & Ritter, H. 1998, *MNRAS*, 293, L42
- Long, M., Romanova, M. M., & Lovelace, R. V. E. 2008, *MNRAS*, 386, 1274
- Markwardt, C. B. & Swank, J. H. 2008, *The Astronomer's Telegram*, 1728
- Papitto, A., di Salvo, T., D'Ai, A., Iaria, R., Burderi, L., Riggio, A., Menna, M. T., & Robba, N. R. 2009, *A&A*, 493, L39
- Patruno, A., Hartman, J. M., Wijnands, R., van der Klis, M., Chakrabarty, D., Morgan, E. H., & Markwardt, C. B. 2008, *The Astronomer's Telegram*, 1760
- Powell, C., Haswell, C., & Falanga, M. 2007, *MNRAS*, 374, 466
- Pringle, J. E. & Rees, M. J. 1972, *A&A*, 21, 1
- Psaltis, D. & Chakrabarty, D. 1999, *ApJ*, 521, 332
- Roche, P., Chakrabarty, D., Morales-Rueda, L., Hynes, R., Slivan, S. M., Simpson, C., & Hewett, P. 1998, *IAU Circ.*, 6885
- Wang, Z., Bassa, C., Cumming, A., & Kaspi, V. M. 2008, *ApJ*, accepted, arXiv: 0812.2815
- Wang, Z., Chakrabarty, D., Roche, P., Charles, P. A., Kuulkers, E., Shahbaz, T., Simpson, C., Forbes, D. A., & Helsdon, S. F. 2001, *ApJ*, 563, L61
- Wijnands, R., Méndez, M., Markwardt, C., van der Klis, M., Chakrabarty, D., & Morgan, E. 2001, *ApJ*, 560, 892
- Wijnands, R. & van der Klis, M. 1998, *Nature*, 394, 344
- Wijnands, R., van der Klis, M., Homan, J., Chakrabarty, D., Markwardt, C. B., & Morgan, E. H. 2003, *Nature*, 424, 44
- Wolff, M. T., Hertz, P., Wood, K. S., Ray, P. S., & Bandyopadhyay, R. M. 2002, *ApJ*, 575, 384

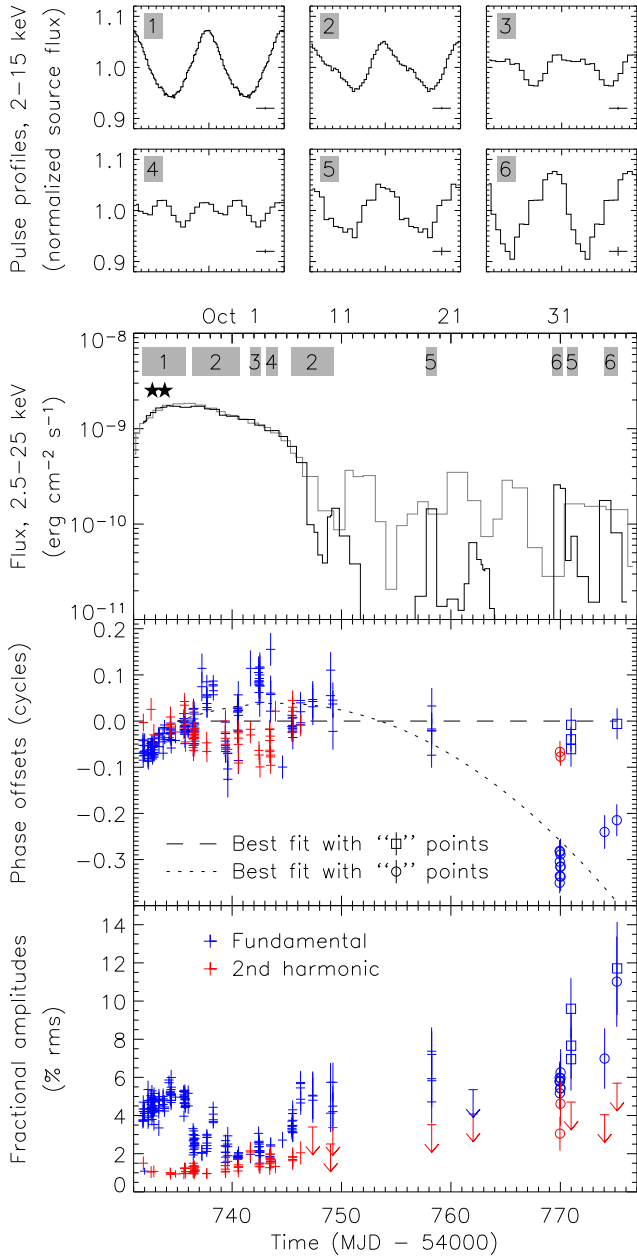


FIG. 1.— The pulse profiles, light curve, phase residuals, and fractional amplitudes for the 2008 outburst of SAX J1808.4–3658. The top panels show the 2–15 keV pulse profiles observed during the outburst. The profiles are background-subtracted and normalized such that the phase bins have a mean value of unity, and the error crosses in the lower right of each graph give the mean uncertainties. Each box shows two cycles, so each minor tick mark on the phase axis is 0.1 cycles. The phases are based on our best-fit constant-frequency spin model. The grey boxes in the light curve plot indicate the time intervals during which the profiles were observed. The second panel shows the light curve of the 2008 outburst, in black. The remarkably similar 2005 outburst is shown in grey for comparison. The stars indicate the times of thermonuclear bursts during 2008. The third panel shows the pulse phase residuals relative to our best-fit constant-frequency model, $\nu = 400.975210133$ Hz. Blue points indicate the phase of the fundamental; red points indicate the second harmonic. Each point represents 512 s of timing data. The phase jumps after MJD 54760 led us to separate the phase measurements as earlier (circles) and later (squares), and the dashed and dotted lines show the respective phase models for each group. The bottom plot shows the fractional amplitudes of the fundamental and harmonic. Arrows give 90% upper limits.

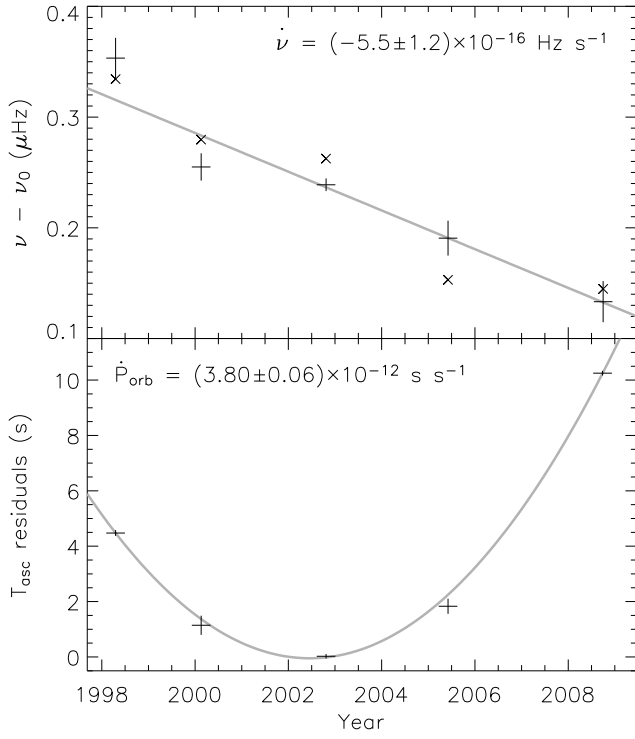


FIG. 2.— The changing spin and orbital timing of SAX J1808.4–3658 during the 1998–2008 outbursts. Top: constant-frequency measurements of each outburst, showing the spin down of the star. The frequencies are relative to $\nu_0 = 400.97521000$ Hz. The \times 's mark what the frequencies would be if the fit source position differed from the actual position by 2σ along the ecliptic plane in the direction of increasing RA. Bottom: the observed times of ascending node, relative to the expected times for a constant period. The T_{asc} of each outburst comes progressively later, indicating a positive orbital period derivative.